JCI The Journal of Clinical Investigation

# A sodium channel knockin mutant ($Na_V1.4$-R669H) mouse model of hypokalemic periodic paralysis

Fenfen Wu, … , Arie F. Struyk, Stephen C. Cannon

*J Clin Invest.* 2011;121(10):4082-4094. https://doi.org/10.1172/JCI57398.

**Research Article** **Muscle biology**

Hypokalemic periodic paralysis (HypoPP) is an ion channelopathy of skeletal muscle characterized by attacks of muscle weakness associated with low serum $K^+$. HypoPP results from a transient failure of muscle fiber excitability. Mutations in the genes encoding a calcium channel ($Ca_V1.1$) and a sodium channel ($Na_V1.4$) have been identified in HypoPP families. Mutations of $Na_V1.4$ give rise to a heterogeneous group of muscle disorders, with gain-of-function defects causing myotonia or hyperkalemic periodic paralysis. To address the question of specificity for the allele encoding the $Na_V1.4$-R669H variant as a cause of HypoPP and to produce a model system in which to characterize functional defects of the mutant channel and susceptibility to paralysis, we generated knockin mice carrying the ortholog of the gene encoding the $Na_V1.4$-R669H variant (referred to herein as R669H mice). Homozygous R669H mice had a robust HypoPP phenotype, with transient loss of muscle excitability and weakness in low-$K^+$ challenge, insensitivity to high-$K^+$ challenge, dominant inheritance, and absence of myotonia. Recovery was sensitive to the $Na^+/K^+$-ATPase pump inhibitor ouabain. Affected fibers had an anomalous inward current at hyperpolarized potentials, consistent with the proposal that a leaky gating pore in R669H channels triggers attacks, whereas a reduction in the amplitude of action potentials implies additional loss-of-function changes for the mutant $Na_V1.4$ channels.



# A sodium channel knockin mutant ($Na_V1.4$-R669H) mouse model of hypokalemic periodic paralysis

Fenfen Wu,[1] Wentao Mi,[1] Dennis K. Burns,[2] Yu Fu,[1] Hillery F. Gray,[1] Arie F. Struyk,[3] and Stephen C. Cannon[1,4]

[1]Department of Neurology and Neurotherapeutics and [2]Department of Neuropathology, UT Southwestern Medical Center, Dallas, Texas, USA. [3]Merck Research Laboratories, North Wales, Pennsylvania, USA. [4]Program in Neuroscience, UT Southwestern Medical Center, Dallas, Texas, USA.

**Hypokalemic periodic paralysis (HypoPP) is an ion channelopathy of skeletal muscle characterized by attacks of muscle weakness associated with low serum $K^+$. HypoPP results from a transient failure of muscle fiber excitability. Mutations in the genes encoding a calcium channel ($Ca_V1.1$) and a sodium channel ($Na_V1.4$) have been identified in HypoPP families. Mutations of $Na_V1.4$ give rise to a heterogeneous group of muscle disorders, with gain-of-function defects causing myotonia or hyperkalemic periodic paralysis. To address the question of specificity for the allele encoding the $Na_V1.4$-R669H variant as a cause of HypoPP and to produce a model system in which to characterize functional defects of the mutant channel and susceptibility to paralysis, we generated knockin mice carrying the ortholog of the gene encoding the $Na_V1.4$-R669H variant (referred to herein as R669H mice). Homozygous R669H mice had a robust HypoPP phenotype, with transient loss of muscle excitability and weakness in low-$K^+$ challenge, insensitivity to high-$K^+$ challenge, dominant inheritance, and absence of myotonia. Recovery was sensitive to the $Na^+/K^+$-ATPase pump inhibitor ouabain. Affected fibers had an anomalous inward current at hyperpolarized potentials, consistent with the proposal that a leaky gating pore in R669H channels triggers attacks, whereas a reduction in the amplitude of action potentials implies additional loss-of-function changes for the mutant $Na_V1.4$ channels.**

## Introduction

Hypokalemic periodic paralysis (HypoPP) is the most prevalent form of familial periodic paralysis and is one of the many ion channelopathies affecting skeletal muscle (1, 2). These rare heritable disorders of muscle present with transient episodes of weakness or muscular stiffness from involuntary after-contractions (myotonia). Both symptoms arise from derangements in the electrical excitability of muscle, as a result of mutations in voltage-gated ion channels that may cause either gain- or loss-of-function changes. Paralysis is caused by a sustained depolarized shift in the muscle resting potential ($V_{rest}$), which inactivates sodium channels and renders the fiber inexcitable. Conversely, myotonia is a state of pathologically enhanced fiber excitability in which bursts of after-discharges persist for several seconds after the cessation of voluntary muscular activity.

In HypoPP, patients have recurrent attacks of weakness in association with low serum $K^+$ (<2.8 mM), but no myotonia (3). The hypokalemia results from a shift of extracellular $K^+$ to the intramuscular space, without a total-body deficit, and paradoxically causes depolarization of $V_{rest}$ (4). The onset of transient attacks occurs near puberty, and many patients develop permanent proximal weakness in late adulthood. The inheritance pattern is autosomal dominant, but with reduced expression of the acute attacks in females (5). Paralytic attacks may be triggered by carbohydrate ingestion, rest after exercise, or emotional stress. Recovery from attacks occurs spontaneously in hours to days, and may be hastened by $K^+$ administration. In some patients, chronic use of $K^+$ supplements or carbonic anhydrase inhibitors will reduce attack frequency and severity (6).

The molecular defect in HypoPP is heterogeneous: 60% of families have missense mutations in *CACNA1S* encoding the L-type calcium channel $Ca_V1.1$, 20% of families have missense mutations in *SCN4A* (encoding the voltage-gated sodium channel $Na_V1.4$), and the remainder are undetermined (5, 7–9). Remarkably, 14 of the 15 HypoPP missense mutations occur at arginine residues in the S4 voltage-sensor domains of $Ca_V1.1$ or $Na_V1.4$ (Figure 1A and ref. 10). Expression studies of HypoPP mutant channels have revealed modest changes in the voltage dependence of channel activation for $Ca_V1.1$ (11) or inactivation for $Na_V1.4$ (12, 13), but these defects could not readily explain the depolarization-induced attacks of weakness in low $K^+$. Subsequent studies in HypoPP $Na_V1.4$ channels revealed an anomalous ion conducting pathway, the gating pore, that enables inward current to flow at $V_{rest}$, at which the S4 voltage sensors are in an inward position that favors closure of the conventional $Na^+$-selective pore (14, 15). The gating pore has been proposed to be the source of current that renders HypoPP fibers susceptible to depolarization in low external $K^+$ (16–18).

Despite these advances in understanding of the molecular genetic basis of HypoPP, much remains to be learned about the mechanistic link between functional defects of mutant channels and susceptibility to attacks of paralysis. Studies in patients are limited for these rare disorders, and the intrinsic variability of symptoms often leads to ambiguous results (19). The $K^+$-depleted rat preparation (20) or $Ba^{2+}$-poisoned muscle fibers (16, 21) have been used as surrogates of HypoPP, but there are no existing genetic models of HypoPP in mammals or lower animals. To address these issues, we developed a mouse model for HypoPP using a targeted mutation in $Na_V1.4$, homologous to the R669H reported for the first family with a HypoPP mutation located in *SCN4A* (8). These mice had

**Conflict of interest:** The authors have declared that no conflict of interest exists.
**Citation for this article:** *J Clin Invest.* 2011;121(10):4082–4094. doi:10.1172/JCI57398.

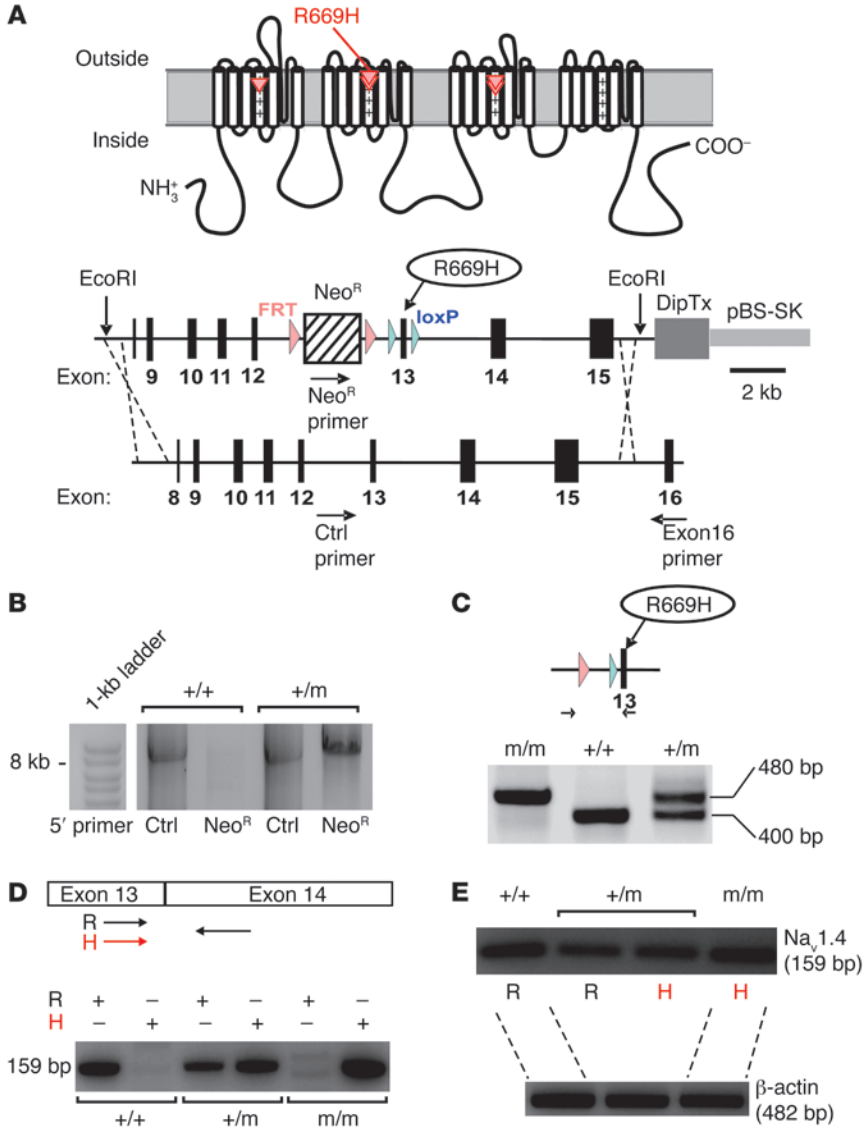


**Figure 1**
Construction and genetic analysis of the $Na_V1.4$-R669H knockin mouse. (**A**) Schematic diagram of $Na_V1.4$ showing the locations of the HypoPP mutations at arginines in S4 voltage sensor domains (red triangles). The targeting construct (22.4 kb) for homologous recombination in mouse *SCN4A* is shown below (see Methods for details). (**B**) PCR amplification of an 8.5-kb fragment from splenic DNA isolated from F1 mice showed integration upstream of exon 16 in *SCN4A*. The reverse primer was in exon 16, downstream from the targeting construct, as shown in **A**. The $Neo^R$ and exon 16 primer pair specifically amplified the $R669H^{+/m}$ allele containing the Neo cassette, but not the WT allele. (**C**) PCR analysis of genomic DNA, after crossing with a line expressing Flp recombinase, showed the removal of the Neo cassette with retention of 1 *FRT* site and 1 *loxP* site upstream of exon 13 (480 bp, compared with 400 bp for WT). The PCR products also demonstrated a homozygous mutant lacking the 400-bp amplimer ($R669H^{m/m}$). (**D**) RT-PCR from muscle total RNA using 40 cycles of amplification showed the specificity of forward primers to amplify only the WT allele R or the mutant allele H. (**E**) Expression levels of WT and mutant alleles were ascertained by RT-PCR for 24 cycles with allele-specific primers, with normalization to expression of the β-actin transcript. Expression of the mutant allele in $R669H^{m/m}$ mice was comparable to that of the WT allele in WT mice, and each allele was present at approximately 70% of total control for $R669H^{+/m}$ mice.

a robust HypoPP phenotype, with loss of muscle excitability and weakness triggered by low $K^+$, dominant inheritance, and absence of myotonia or paralysis in high $K^+$.

## Results

*Generation of $Na_V1.4$-R669H mice*. The R669H mutation in human $Na_V1.4$ associated with HypoPP was introduced to the mouse ortholog ($mNa_V1.4$-R663H) by homologous recombination using a 22.4-kb targeting vector, pNAR663H, containing exons 8–15 (Figure 1A). The arginine-to-histidine HypoPP mutation in exon 13 was paired with silent polymorphisms at codons 661 and 662 to aid in genotyping by PCR and restriction digest. Resistance to neomycin was used to screen for recombination in 129/Sv ES cells, and blastocyst injection was performed by the UT Southwestern Transgenic Core Facility. Founder mice had a high degree of chimerism, and germline transmission with recombination of the targeting construct at the correct site in F1 progeny was confirmed by PCR amplification of an 8.5-kb product from splenic DNA using a forward primer at a unique site in pNAR663H and a reverse primer in exon 16 located downstream from the targeting sequence (Figure 1B). Sequence analysis confirmed the presence of the murine R663H mutation and correct alignment of the recombination event upstream of exon 16. For consistency with the literature on HypoPP in humans, the heterozygous $SCN4A^{+/R669H}$ and homozygous $SCN4A^{R669H/R669H}$ mutant mice are referred to herein as $R669H^{+/m}$ and $R669H^{m/m}$, respectively.

The F1 $R669H^{+/m}$ mice were viable, developed normally, and bred successfully. To excise the *FRT*-flanked neomycin resistance gene from intron 12, we crossed a $R669H^{+/m}$ male with a female 129/Svflip1 mouse that constitutively expresses Flp recombinase. All subsequent breeding was in the 129/Sv strain, with the neomycin-deleted line. Genotyping was performed by PCR amplification of genomic DNA with a primer pair that spanned the intron 12/exon 13 boundary (Figure 1C). The retained intronic *FRT* and *loxP* sites in the mutant allele produced a 480-bp product that was distinguishable from the 400-bp WT amplimer. Genotyping at 4 weeks of age revealed the mutant allele at the expected Mendelian frequencies. In matings between WT and $R669H^{+/m}$ mice, the

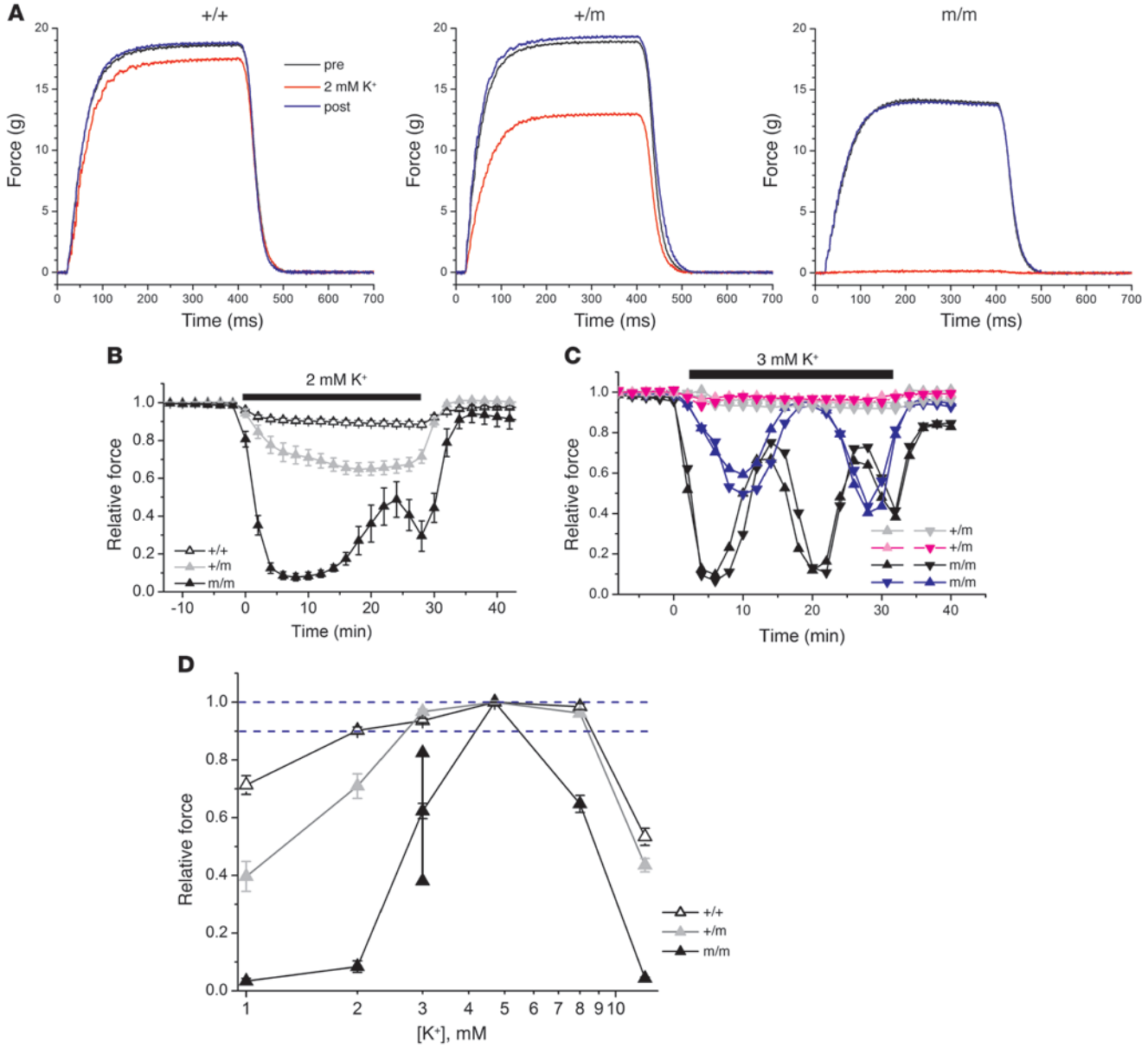


**Figure 2**

In vitro contraction testing demonstrates a HypoPP phenotype. (**A**) Force tracings of isometric tetanic contractions recorded in standard bath solution (4.75 mM $K^+$; black), after 10 minutes in 2 mM $K^+$ (red), and after recovering in standard solution for 10 minutes (blue). $R669H^{+/m}$ and $R669H^{m/m}$ mice were more susceptible to hypokalemic-induced weakness. The baseline tetanic force was consistently lower in $R669H^{m/m}$ mice. (**B**) Average responses for a 30-minute exposure to 2 mM $K^+$ challenge ($n$ = 10 [WT]; 8 [$R669H^{+/m}$ and $R669H^{m/m}$]). Tetanic force was recorded every 2 minutes and for each muscle and was normalized to the control response preceding the hypokalemic challenge. (**C**) Response to 3 mM $K^+$ challenge, presented as paired recordings from individual soleus muscles from the left and right hindlimbs (tested in separate tissue baths). Paired muscles from the same animal are shown by symbol color. Large-amplitude oscillations in force were observed for all $R669H^{m/m}$ muscles tested ($n$ = 10). The pair of recordings from 2 different $R669H^{m/m}$ mice illustrates the highly synchronous responses for muscles harvested from the same animal. (**D**) Dose-response relation for tetanic contraction after a 10-minute exposure to varying levels of $K^+$. Average maximum and minimum forces observed during 30 minutes' exposure are also indicated (vertical lines). For $R669H^{+/m}$ mice, increased susceptibility to weakness was observed at low $K^+$, but not for high $K^+$ as occurs in HyperPP. Dashed lines span the top 10% of relative force.

offspring were 52% WT and 48% $R669H^{+/m}$ ($n$ = 151). When heterozygote pairs were bred, the offspring were 21% WT, 30% $R669H^{m/m}$, and 49% $R669H^{+/m}$ ($n$ = 139).

Expression of the mutant allele was detected by RT-PCR amplification with a primer pair that spanned the exon 13/14 junction. Allele-specific forward primers were designed to selectively amplify first-strand cDNAs synthesized from WT or R669H transcripts. Specificity was demonstrated in Figure 1D; the mutant allele primer H failed to amplify a product from WT cDNA, whereas the WT primer R failed to generate a product from

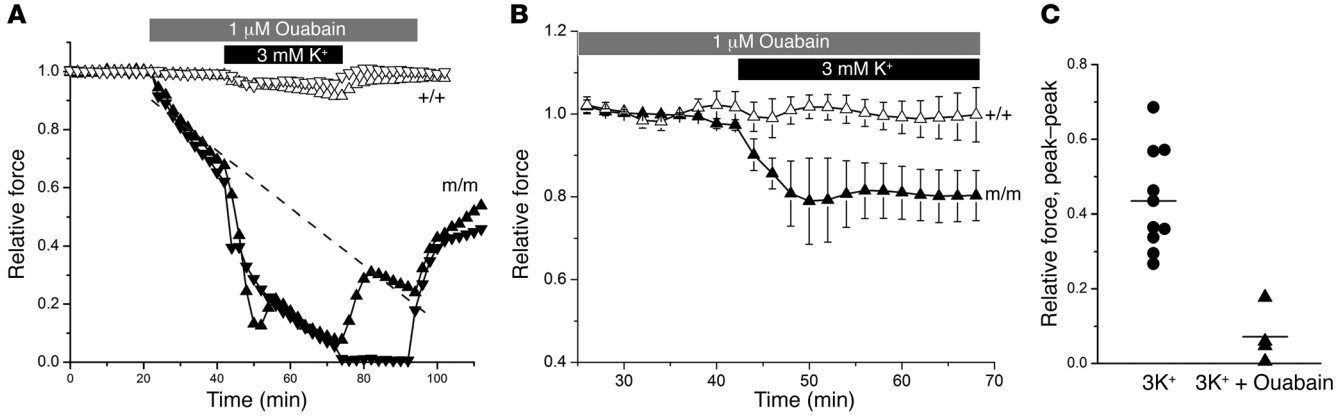


**Figure 3**

Recovery from weakness was ouabain sensitive. In vitro contraction responses from R669H$^{m/m}$ muscle exposed to 3 mM K$^+$ were used to assess whether spontaneous recovery of force during hypokalemia was ouabain sensitive. (**A**) Pretreatment with 1 μM ouabain caused a decline in force for R669H$^{m/m}$, but not WT, muscle. Concurrent exposure to 3 mM K$^+$ produced a further decline in force and suppressed large oscillation in force. Responses are from 2 individual soleus muscles harvested from R669H$^{m/m}$ or WT mice. (**B**) Compensation for the ouabain-induced decline in force (dashed line in **A**) revealed the persistence of hypokalemia-induced weakness, but with suppression of spontaneous recovery. Responses are averages ($n$ = 4 [R669H$^{m/m}$]; 2 [WT]). (**C**) Peak-to-peak amplitude for the spontaneous oscillation in R669H$^{m/m}$ soleus force during 3 mM K$^+$ challenge, shown for 10 separate muscles without ouabain and for 4 muscles pretreated with 1 μM ouabain.

R669H$^{m/m}$ cDNA. The abundance of each transcript was estimated from the OD of each allele-specific product after 24 cycles of amplification, normalized to a control product amplified from β-actin (Figure 1E). Transcript levels for WT and R669H alleles in R669H$^{+/m}$ mice were 0.71 and 0.72, respectively, relative to $Na_V1.4$ transcript expression in WT mice, and that for the mutant allele in R669H$^{m/m}$ mice was 0.98.

*R669H mice appear normal.* Viability of R669H$^{+/m}$ and R669H$^{m/m}$ mice was indistinguishable from that of WT animals, consistent with the frequency distribution of genotypes observed at 4 weeks of age. Body mass was measured weekly from 4 to 52 weeks of age for WT and R669H$^{+/m}$ mice, and no difference was observed ($P$ > 0.3, $n$ = 9 per genotype; Supplemental Figure 1; supplemental material available online with this article; doi:10.1172/JCI57398DS1). Mutant mice, R669H$^{+/m}$ or R669H$^{m/m}$, had normal locomotor activity, without visibly apparent myotonic stiffness or spontaneous attacks of weakness. Quantitative grip strength testing showed a modest trend for hindlimb weakness, with approximately 10% reduction in maximal force for R669H$^{+/m}$ versus WT, for both male and female mice ages 8–12 months, but this was not statistically significant ($n$ = 8; $P$ > 0.1; Supplemental Figure 1). No difference was observed in forelimb grip strength.

*In vitro contraction testing reveals a HypoPP phenotype.* Spontaneous attacks of weakness in human periodic paralysis occur with high variability in frequency and severity, and even provocative maneuvers do not always trigger an attack (1). In vitro contraction testing by hypokalemic challenge is a more reliable method to provoke a reduction of peak force in HypoPP muscle. Moreover, local extracellular K$^+$ concentration can be controlled more easily and with greater accuracy in the tissue bath than can be achieved in vivo.

Isometric tetanic contractions were measured for soleus muscle maintained at 37°C in a tissue bath. Contractions were elicited by direct field stimulation of muscle fibers using parallel wire electrodes (2-ms pulses, 100 Hz; $n$ = 40), and the bath contained curare (0.25 μM) to block neuromuscular transmission from activation of terminal branches of motor axons. In the standard bath containing 4.75 mM K$^+$, the baseline force was reduced for R669H$^{m/m}$ mice (12.3 ± 0.49 g; $n$ = 33; $P$ < 0.0001) compared with R669H$^{+/m}$ (16.3 ± 0.38 g; $n$ = 36) or WT (15.7 ± 0.37 g; $n$ = 41). Force transients recorded in the standard bath, after 10 minutes in a 2 mM K$^+$ challenge, and then 10 minutes after return to control are shown for representative individual soleus muscles from each genotype in Figure 2A. Muscle from the R669H mice had increased susceptibility to loss of force generation in 2 mM K$^+$ that was more severe for R669H$^{m/m}$ than R669H$^{+/m}$ mice. The kinetics for the rise and decay of force transients were mildly slowed for R669H$^{m/m}$ soleus during episodes of weakness in low K$^+$, but there was no evidence of prolonged after contractions that are characteristic of myotonia.

The time course of the onset and recovery from a loss of muscle force during a 30-minute exposure to 2 mM K$^+$ is shown as averaged responses from 8–10 muscle preparations per genotype in Figure 2B. The effect of R669H gene dosage is reflected by the nadir in force during the hypokalemic challenge, with that for R669H$^{m/m}$ less than that for R669H$^{+/m}$. Partial recovery in force for R669H$^{m/m}$ muscle occurred during the 2 mM K$^+$ interval, as shown by the force increase after 15 minutes. In 4 of 9 R669H$^{m/m}$ fibers, the force recovered to greater than 50% of baseline during the hypokalemic challenge, but the asynchronous timing of recovery caused an attenuation of the mean response with an increased SEM. With a 3 mM K$^+$ challenge, severe loss of force was again triggered for R669H$^{m/m}$ soleus, but the recovery during hypokalemia was dramatically more prominent than that with 2 mM K$^+$ (Figure 2C). All 10 R669H$^{m/m}$ muscles tested showed pronounced oscillations in force with recovery and then recurrent loss during a 30-minute challenge in 3 mM K$^+$. The period of the oscillations was similar for all muscles, with a mean of 16.8 ± 1.1 minutes ($n$ = 10), whereas the amplitude was more variable (Figure 2C). In all cases, the behavior was remarkably similar for paired left and right muscles from the same animal (albeit tested in separate tissue baths) compared with responses in muscles from other animals. This pattern suggests that the response to hypokalemia is

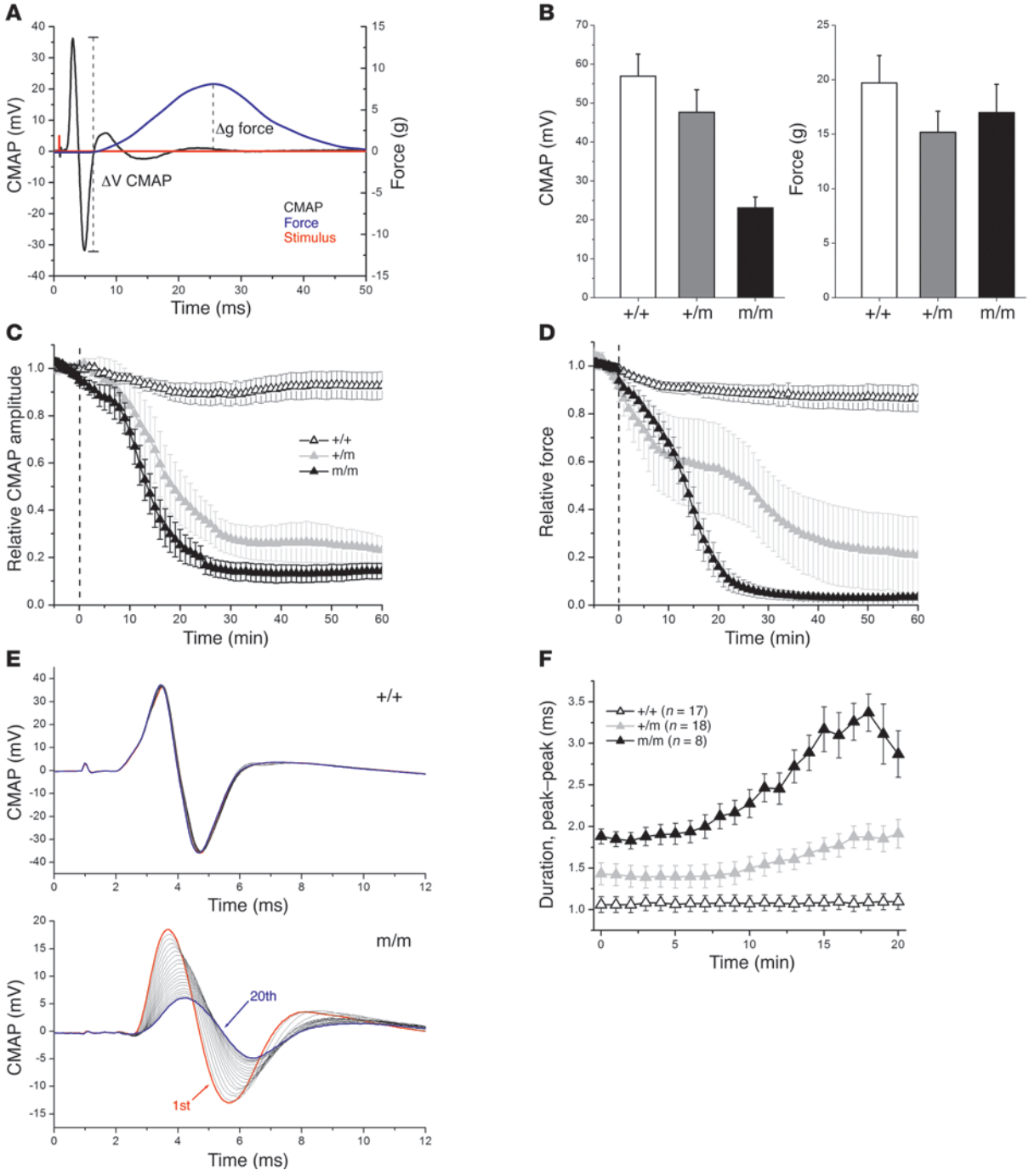


**Figure 4**

In vivo reduction of muscle excitability and force from glucose plus insulin challenge. (**A**) CMAP (black) and force (blue) at the Achilles tendon were recorded simultaneously in response to a single 0.1-ms shock (red) applied to the sciatic nerve. Sample tracings are from a single trial (nonaveraged) recorded from a R669H$^{+/m}$ mouse. (**B**) Baseline CMAP amplitude and force, recorded before glucose plus insulin infusion. Relative change in CMAP amplitude (**C**) and twitch force (**D**) in response to glucose and insulin infusion. Amplitudes were normalized to the average of 5 trials before the start of the infusion (vertical dashed lines). (**E**) Individual CMAP responses are superimposed for the first 20 responses, measured at 1-minute intervals, after glucose plus insulin infusion for WT and R669H$^{m/m}$ animals. (**F**) The duration of the CMAP (peak to peak) was prolonged for R669H mutants and increased during glucose plus insulin infusion. (**B**–**D**) Responses are averaged ($n$ = 16 [WT]; 8 [R669H$^{+/m}$]; 7 [R669H$^{m/m}$]).

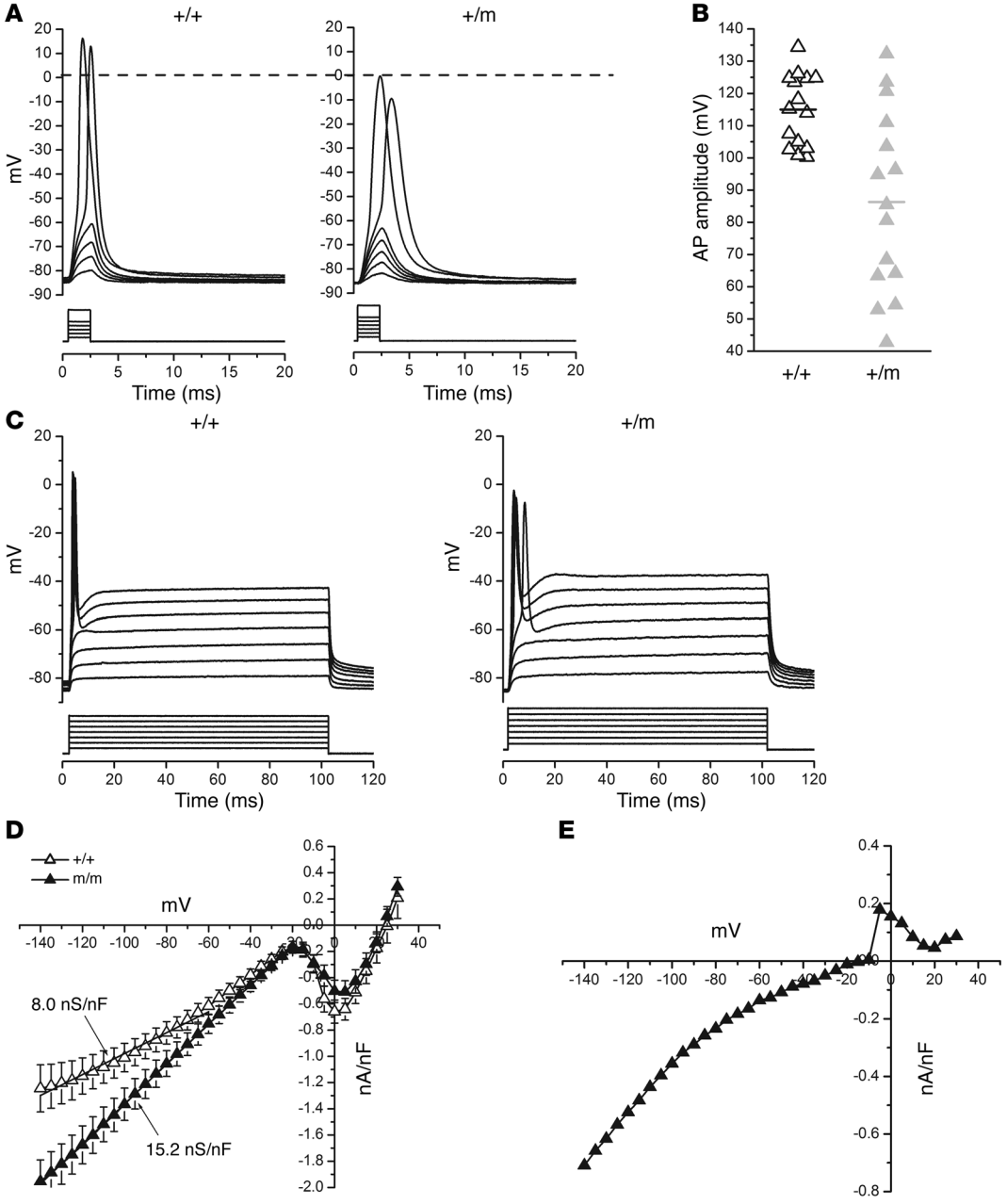


**Figure 5**

Reduced muscle excitability in R669H fibers. (**A**) Muscle voltage responses elicited by a series of 2-ms stimuli at progressively larger current amplitudes. A holding current was applied to set the initial membrane potential at –85 mV. Action potentials peaked with an overshoot greater than 0 mV (dashed line) for WT fibers, but not for all R669H$^{+/m}$ fibers. Maximal current stimulus was 1.5× threshold. (**B**) Action potential (AP) amplitudes elicited by 1.5× threshold stimuli were smaller for R669H$^{+/m}$ than WT fibers ($n$ = 15 fibers from 5 muscle preparations per genotype). (**C**) Voltage transients in response to 100-ms stimulating current injections. A single action potential was elicited in both WT and R669H$^{+/m}$ fibers, even for stimulus currents of 1.5× threshold, demonstrating an absence of myotonia. (**D**) Voltage dependence for the steady-state current recorded at the end of a 300-ms voltage pulse revealed an increased inward (negative) current for R669H$^{m/m}$ fibers. Currents are the lanthanum-sensitive component determined by subtraction of those recorded in a bath containing 3.5 mM $La^{3+}$ from control responses. Inflection between –30 mV and +20 mV reflects a residual $Ca^{2+}$ current blocked by $La^{3+}$. (**E**) Subtraction of La-sensitive currents in WT fibers from R669H$^{m/m}$ yielded the gating pore current that was activated at hyperpolarized potentials.

highly consistent, but that the basal state of susceptible muscles varied from animal to animal in an unpredictable fashion, possibly related to the recent level of motor activity or food ingestion immediately prior to the study.

The dose-response relation for $K^+$-induced weakness is shown in Figure 2D. The force measured 10 minutes after initiation of the $K^+$ challenge was selected to define the dose-response relation, since this time point reflects the extent of force reduction before recovery

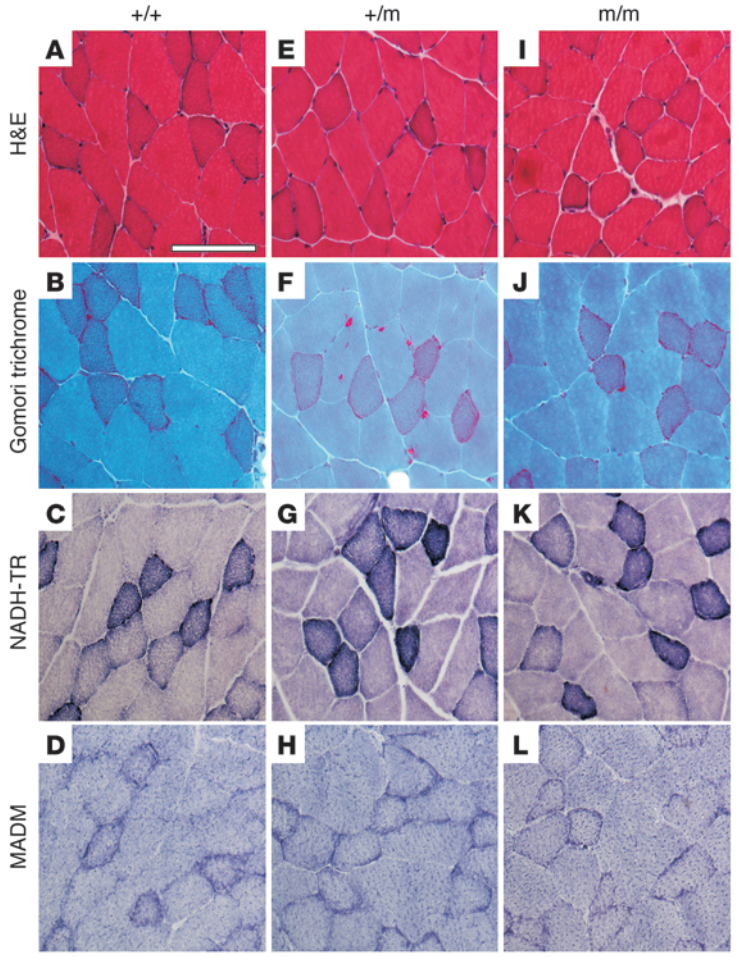


**Figure 6**
Histological analysis of quadriceps muscles. Frozen blocks were sectioned at 10-μm thicknesses and stained with H&E (**A**, **E**, and **I**), Gomori trichrome (**B**, **F**, and **J**), nicotinamide adenine dehydrogenase-tetrazolium reductase (NADH-TR; **C**, **G**, and **K**), and myoadenylate deaminase (MADM; **D**, **H**, and **L**). Red-staining subsarcolemmal inclusions on Gomori trichrome (**F** and **J**) were the only changes observed for R669H mutant muscle. Scale bar: 50 μm.

or oscillations ensued. WT soleus muscle tolerated a wide range in extracellular $K^+$ from 2 to 8 mM with less than a 10% reduction in tetanic isometric force. For $R669H^{+/m}$ soleus, a model for the mutant allele dosage in human HypoPP, susceptibility to loss of force was markedly increased by hypokalemia at $K^+$ of 2 mM ($P < 0.0005$) and 1 mM ($P < 0.0001$) compared with WT. Conversely, the responses at 8 and 12 mM $K^+$ were not different from WT. The $K^+$ sensitivity of $R669H^{+/m}$ muscle showed a clear HypoPP phenotype. These data provide the first comprehensive dose-response relation to our knowledge in support of HypoPP arising from a mutation in $Na_V1.4$. Importantly, these data also show that $R669H^{+/m}$ mice do not have an increased susceptibility to force reduction in high $K^+$. This distinction is notable because other disease-associated mutations in $Na_V1.4$ with gain-of-function alterations in channel activity will predispose muscle to attacks of hyperkalemic periodic paralysis (HyperPP), often accompanied with myotonia (22). $R669H^{m/m}$ muscle was more susceptible to a severe loss of force, in either low or high $K^+$. Because spontaneous oscillations in muscle force were so prominent for $R669H^{m/m}$ soleus in 3 mM $K^+$, we depicted the response in Figure 2D as the mean value recorded at 10 minutes ($n = 6$), with dashed lines denoting the average maximum and minimum forces observed during the 30-minute exposure.

The carbonic anhydrase inhibitor acetazolamide (ACTZ) reduces the frequency and severity of paralytic attacks in some patients with periodic paralysis. Moreover, we have previously demonstrated the efficacy of 100 μM ACTZ in suppressing the reduction of force by hyperkalemic challenge in the $Na_V1.4$-M1592V HyperPP mouse (23). Paired testing of control or pretreatment with 200 μM ACTZ for 30 minutes in $R669H^{+/m}$ muscles from the EDL ($n = 4$) or soleus ($n = 5$) failed to reveal protection from weakness during a 2 mM $K^+$ challenge in 8 of 9 trials.

*Recovery from loss of force is ouabain sensitive*. The robust occurrence of oscillations in muscle force during a 3 mM $K^+$ challenge for $R669H^{m/m}$ muscle (Figure 2C) provided an opportunity to investigate the basis for recovery from an attack of periodic paralysis, independent of shifts in serum $K^+$. Because depolarization of $V_{rest}$ is the proximate cause of weakness during an attack of HypoPP (4), we reasoned that compensation from the $Na^+/K^+$-ATPase pump might be required to repolarize fibers. Pilot experiments showed that normal mouse soleus can tolerate the pump inhibitor ouabain up to a concentration of 1 μM without a loss of muscle force over a 30-minute observation period. Therefore, we tested whether pretreatment with 1 μM ouabain would block recovery in muscle force for $R669H^{m/m}$ soleus during a subsequent exposure to 3 mM $K^+$. Responses for a pair of WT and $R669H^{m/m}$ muscles from 2 animals are shown in Figure 3A. Unlike WT muscle, the $R669H^{m/m}$ soleus did not tolerate 1 μM ouabain in the standard bath containing 4.75 mM $K^+$ (20- to 40-minute interval). This suggested that $R669H^{m/m}$ soleus has an increased dependency on pump activity to maintain $V_{rest}$ and excitability, even in normal $K^+$. Hypokalemic challenge with 3 mM $K^+$ produced a further reduction in force for $R669H^{m/m}$ muscle and dramatically suppressed the oscillation in force; some fibers failed to recover even after the $K^+$ was returned to 4.75 mM (Figure 3A). Recovery ensued only after the ouabain was washed out (90–110 minutes). To isolate the $K^+$-dependent component of the force for $R669H^{m/m}$ fibers in the presence of ouabain, we subtracted the linear decay of force in 1 μM ouabain while in standard bath solution. The average behavior recorded from 4 $R669H^{m/m}$ fibers demonstrated that the hypokalemia-induced reduction in force was still discernable in the presence of 1 μM ouabain, but that recovery did not occur over a 30-minute observation period in 3 mM $K^+$ (Figure 3B). The variability in force responses from individual fibers is illustrated in Figure 3C. Large amplitude peak-to-peak oscillations in relative force were observed for all 10 $R669H^{m/m}$ fibers exposed to 3 mM $K^+$ (relative value 0.44 ± 0.043), whereas in 4 other $R669H^{m/m}$ muscles tested, the presence of 1 μM ouabain the amplitude was greatly diminished (relative value 0.073 ± 0.037; $P < 0.0005$).

*In vivo loss of muscle excitability and force from glucose plus insulin challenge*. Susceptibility to an attack of HypoPP in vivo was investigated by inducing hypokalemia with a continuous infusion of glucose plus insulin. Pilot experiments revealed a large variability in responses, with onset of weakness varying from 10 to 60 minutes after the

start of the infusion and with the severity of force reduction ranging from 50% to 90% or even some failures. In an effort to achieve greater consistency in the responses, we used a pharmacologic approach to establish a common starting point for the extracellular $K^+$. Basal hypokalemia was induced by pretreatment for 48 hours with an oral K-binding resin, sodium polystyrene sulfonate, which reduced serum $K^+$ to 2.79 ± 0.21 mM (WT), 2.65 ± 0.07 mM ($R669H^{+/m}$), and 2.24 ± 0.08 mM ($R669H^{m/m}$), but did not result in attacks of weakness detectable by observing motor behavior. These mice were then stably anesthetized for hours by isoflurane inhalation, and the glucose plus insulin mixture was administered intravenously (0.5 ml/h) at the jugular vein. Contraction was elicited by a single shock applied to the sciatic nerve. Muscle excitability was monitored as the compound muscle action potential (CMAP), recorded extracellularly with an electromyography needle positioned in the gastrocnemius or soleus muscles. The Achilles tendon was severed and attached to a force transducer to monitor muscle contraction. At the end of the 2-hour infusion, serum $K^+$ decreased within each genotype and was significantly lower for $R669H^{m/m}$ compared with WT mice (1.51 ± 0.14 mM vs. 2.25 ± 0.13 mM; $P < 0.05$), whereas $R669H^{+/m}$ mice showed a similar trend that did not reach statistical difference (1.97 ± 0.34 mM; $P = 0.07$, ANOVA with Bonferroni correction).

Figure 4A shows an example of the primary data, with a simultaneous measurement of CMAP amplitude and peak muscle force. The baseline CMAP amplitude, after sodium polystyrene sulfonate but before insulin infusion, was reduced for $R669H^{m/m}$ compared with WT or $R669H^{+/m}$ mice ($P < 0.05$; Figure 4B). Basal twitch force, however, did not differ among the various genotypes. The CMAP and peak twitch force were measured every minute over a 1-hour period of glucose plus insulin infusion. In R669H mutant muscle, the relative amplitudes for these measures of muscle electrical excitability and mechanical contraction decreased markedly within minutes of starting the infusion (Figure 4, C and D), whereas WT muscle was relatively unaffected. As with the in vitro contraction test (Figure 2), a gene dosage effect was apparent, with the decline in CMAP and force being more rapid and more extensive for $R669H^{m/m}$ than for $R669H^{+/m}$ soleus.

In addition to the R669H effects on amplitude, the shape of the CMAP waveform was altered for HypoPP muscle. CMAP duration was increased at baseline, before the glucose plus insulin infusion (WT, 1.06 ± 0.09 ms, $n = 17$; $R669H^{+/m}$, 1.43 ± 0.13 ms, $n = 18$; $R669H^{m/m}$, 1.88 ± 0.09 ms, $n = 8$; $P < 0.001$). During the infusion, CMAP duration became further prolonged in R669H mice, whereas the CMAP waveform was stable in WT animals (Figure 4E). The time course for the prolongation of CMAP duration over the first 20 minutes of the infusion is shown in Figure 4F. The increase in CMAP duration occurred with a lag of about 8 minutes, similar to the lag for the decrement in CMAP amplitude and twitch force (Figure 4, B and C). On average, nearly a 3-fold increase in CMAP duration was observed during glucose plus insulin infusion for $R669H^{m/m}$ muscle.

*Muscle fiber excitability of R669H mice.* Attacks of weakness in HypoPP are caused by transient impairment of muscle fiber excitability, which in turn is derived from a failure to maintain $V_{rest}$ (4). $V_{rest}$ was measured by impalement of fibers from whole soleus muscle maintained in vitro at 37°C. In 4.75 mM $K^+$, $V_{rest}$ was comparable for 501 WT and 456 $R669H^{+/m}$ fibers (–72.6 ± 0.66 and –73.6 ± 0.41 mV, respectively; $P = 0.21$). Upon reducing the bath $K^+$ to 2 mM, however, the values diverged: WT fibers hyperpolarized by –9 mV to –81.7 ± 0.82 mV, as expected, whereas $R669H^{+/m}$ fibers depolarized mildly by +3 mV to –70.6 ± 0.40 mV, with a net result that in 2 mM $K^+$, $R669H^{+/m}$ fibers were depolarized by 11 mV compared with WT ($P < 0.001$).

In addition to the effect on $V_{rest}$, the intrinsic excitability of R669H HypoPP fibers was reduced. Current clamp recording with 2 microelectrodes was used to elicit action potentials from a fixed holding potential of –85 mV. Action potentials in $R669H^{+/m}$ fibers often failed to overshoot 0 mV, in contrast to responses in WT fibers, for which every trial had a peak greater than 0 mV (Figure 5A). Responses were compared quantitatively as the amplitude of the action potential elicited by a 2-ms current injection of 1.5× threshold intensity. The action potential amplitude was larger for WT than for $R669H^{+/m}$ fibers (115 ± 2.9 mV vs. 86.3 ± 7.3 mV; $n = 15$ per group; $P < 0.005$; Figure 5B). The half-amplitude duration was prolonged in $R669H^{+/m}$ fibers (1.3 ± 0.2 ms vs. 0.78 ± 0.05 ms in WT; $P < 0.005$). The maximum rate of rise for the action potential ($dV/dt$) was reduced in $R669H^{+/m}$ fibers (253 ± 49 mV/ms vs. 389 ± 24 mV/ms in WT; $P < 0.05$). There was no difference in the voltage threshold ($R669H^{+/m}$, –56.4 ± 1.4 mV; WT, –55.0 ± 1.0 mV) or stimulus current threshold ($R669H^{+/m}$, 141 ± 10 nA; WT, 141 ± 11 nA).

To assess the susceptibility to firing bursts of myotonic discharges, current clamp recordings were performed with a 100-ms stimulus (Figure 5C). For both WT and $R669H^{+/m}$ fibers, only a single action potential was elicited as the current intensity was increased up to 1.5× threshold. The absence of myotonic bursts of discharges was consistent with the normal relaxation times for the in vitro contraction measurements (Figure 2B), which demonstrated that the R669H mutation does not cause myotonia.

Expression studies of $Na_V1.4$-R669H (rat isoform) in frog oocytes have demonstrated an anomalous inward current at potentials more negative than –20 mV, in which the voltage sensor is biased toward the inward conformation that favors channel closure (15). This gating pore current flows through an accessory pathway created by the misfit between the voltage sensor and the channel complex and has been proposed to be the cause of aberrant depolarization during an attack of paralysis. To confirm the presence of the gating pore current in affected mouse fibers, we recorded steady-state currents in voltage-clamp studies of fibers dissociated from the footpad (flexor digitorum brevis and lumbricales). Blockers were used to suppress $Na^+$, $K^+$, and $Ca^{2+}$ currents, and a chloride-free extracellular solution was used to suppress the $Cl^-$ current. The residual current was still large (~5 nA/nF at –100 mV) compared with the predicted amplitude of the gating pore current (~1 nA/nF), and so the sensitivity for detection was further increased by extracting the component of current blocked by 3.5 mM lanthanum, which produces approximately 65% block of the gating pore current (24). Fibers from $R669H^{m/m}$ mice showed an increased inward current at test potentials more negative than –20 mV compared with those from WT mice (Figure 5D). The slope conductance was increased for $R669H^{m/m}$ compared with WT fibers (15.2 ± 1.2 nS/nF vs. 8.0 ± 1.6 nS/nF; $n = 14$ per group; $P = 0.011$), suggestive of a gating pore conductance of 7 nS/nF at $V_{rest}$ of –90 mV. The difference between these 2 current-voltage curves revealed the typical current-voltage profile of a gating pore current activated at hyperpolarized potentials (Figure 5E).

*Histological features of R669H mice.* Quadriceps muscles from WT, $R669H^{+/m}$, and $R669H^{m/m}$ adult mice aged 8–12 months were evaluated histologically (Figure 6). Muscles from both $R669H^{+/m}$ and $R669H^{m/m}$ mutants revealed modest, nonspecific changes compared with WT fibers in the form of occasional red-staining subsarcolem-

mal inclusions of uncertain origin in the Gomori trichrome stain (Figure 6, F and J). Similar subsarcolemmal accumulations were observed in type 2 fibers from 2 patients with HypoPP caused by the $Na_V1.4$-R672G mutation and were attributed to transverse tubular aggregates (9). Ultrastructural evaluation revealed very slight dilatation of sarcoplasmic triads in R669H$^{m/m}$ animals (data not shown), but no other abnormalities. Vacuolar changes were not found in the R669H mouse fibers, nor in the human HypoPP $Na_V1.4$-R672G specimens, which was remarkable because vacuoles are commonly a prominent feature of biopsies from patients with HypoPP caused by mutations in $Ca_V1.1$ (9).

## Discussion

A targeted point mutation in the mouse skeletal muscle sodium channel corresponding to human R669H resulted in a phenotype that recapitulated the major features of HypoPP. These features in common with all forms of HypoPP (1) included: (a) transient loss of muscle excitability and severe weakness triggered by low extracellular $K^+$, (b) autosomal-dominant transmission, (c) normal strength between attacks, and (d) absence of myotonia. Moreover, distinctive features of HypoPP found in patients with mutations of $Na_V1.4$, but not of $Ca_V1.1$, were also observed in our R669H mice. First, vacuolar myopathy was notably absent in our R669H mice, as was the case for the HypoPP family in the initial report of R669H (8) and for patients with the $Na_V1.4$-R672G mutation (9), whereas for $Ca_V1.1$ HypoPP, vacuolar changes are prominent (25). Second, the penetrance of susceptibility to weakness with low-$K^+$ challenge was equal in male and female mice, which has been reported as another distinguishing feature of $Na_V1.4$ HypoPP, whereas with $Ca_V1.1$ mutations, the phenotypic expression of transient attacks is reduced in females (5, 9). Third, ACTZ was not effective in preventing the low $K^+$–induced loss of force for the in vitro contraction test. Similarly, patients with $Na_V1.4$ HypoPP do not benefit from ACTZ or may even have exacerbation of paralytic attacks, whereas most patients with $Ca_V1.1$ HypoPP have a reduction of attacks with ACTZ treatment (9). We did not observe spontaneous attacks of weakness, even after oral challenge with sodium polystyrene sulfonate to reduce serum $K^+$. Subclinical impairment of muscle excitability did occur, however, as demonstrated by the reduction in baseline CMAP for R669H$^{m/m}$ mice (Figure 4B). It should also be noted that some patients with HypoPP experience only a few attacks during a lifetime, and the frequency of spontaneous attacks may be lower in HypoPP from $Na_V1.4$ mutations than in that from $Ca_V1.1$ mutations (18). An attack in our mice may have been missed, since continuous 24-hour video monitoring was not performed, nor was provocative testing with forced exercise attempted. Regardless, our observations on the phenotype of R669H mice provide compelling evidence that this missense mutation in $Na_V1.4$ is sufficient to cause HypoPP.

*Modulation of excitability in HypoPP fibers*. The availability of an animal model for $Na_V1.4$ HypoPP provides an intriguing opportunity to characterize the interaction between environmental stresses and susceptibility to loss of excitability with weakness. The strong coupling between these triggers and muscle excitability is a notable feature in all forms of familial periodic paralysis (1, 3), and a greater understanding of these phenomena will provide insights into the disease mechanism. These questions cannot be addressed in cell-based models. Moreover, the scarcity and brief viability of human muscle biopsy specimens places severe constraints on the use of human tissue to address these questions experimentally.

The dose-response relation for the in vitro studies of $K^+$ and tetanic force (Figure 2D) establishes a benchmark that has not, to our knowledge, been previously available for any form of periodic paralysis. Overall, the present data showed that mice heterozygous for the $Na_V1.4$-R669H allele, analogous to the human disorder, had increased susceptibility to weakness in low $K^+$, but not high $K^+$, thereby establishing an unequivocal HypoPP phenotype. These data also established a threshold between 3 and 2 mM $K^+$ at which R669H$^{+/m}$ fibers became detectably weak. Another result from the in vitro contraction studies was the remarkable similarity in the responses for paired muscles isolated from the left and right hindlimbs of a single animal (tested in separate organ baths). The close correlation was shown by the slow oscillations in force amplitude (Figure 2C), but the same phenomenon was observed for monophasic responses and for muscle from R669H$^{+/m}$ as well as R669H$^{m/m}$ mice. We interpret this observation as evidence that a robust and highly reproducible relation exists between susceptibility to weakness and an environmental trigger. We suggest that the notoriously high degree of variability in HypoPP patient responses to controlled provocative challenges (1), or in functional studies on biopsies from patients with periodic paralysis (19), is derived from differences in the initial state or set point of the muscle that are either not controllable or unknown. Our mouse studies showed that when 2 muscles were at the same initial state, there was very little stochastic variability in the HypoPP response.

The dosage of the mutant R669H allele had a pronounced effect on muscle excitability and force. Compared with the in vitro contraction responses for R669H$^{+/m}$ muscle, for R669H$^{m/m}$ muscle, the onset of weakness occurred with a milder reduction in $K^+$ (3 mM vs. 2 mM), and the severity of weakness was more pronounced. The in vivo studies showed a similar dosage effect in R669H$^{m/m}$ animals (Figure 4), with reduced baseline CMAP amplitude, a more rapid onset and greater extent of excitability loss and weakness with glucose plus insulin challenge, and greater prolongation of CMAP amplitude. Remarkably, a case of homozygosity for the $Na_V1.4$-R1132Q mutation has been reported in a family with HypoPP (26). Similar to our animal studies, the clinical phenotype and CMAP studies both showed more severe changes. These observations imply an incomplete dominance for the inheritance of $Na_V1.4$ HypoPP, in that function was not completely abrogated by a single copy of the mutant allele. This pattern was consistent with the notion that the R669H causes a gain-of-function defect, the leak in the gating pore current (14, 15). The current density resulting from expression of 1 mutant allele was sufficient to cause HypoPP, but the deleterious effect was not saturated. Doubling the gating pore current by expression of a second mutant allele further increased susceptibility to attacks of HypoPP.

The in vitro contraction studies revealed slow, large-amplitude oscillations in tetanic force for $K^+$ levels at the transition zone between normal and susceptibility to marked weakness. This transition was at 2 mM for R669H$^{+/m}$ muscle and 3 mM for R669H$^{m/m}$ muscle. The oscillatory behavior in R669H$^{m/m}$ animals was surprisingly robust in that it occurred for all 10 muscles tested. This consistency provided an opportunity to probe the mechanism by which affected muscle recovers from an attack of periodic paralysis. The $Na^+/K^+$-ATPase pump inhibitor ouabain suppressed the oscillations (Figure 3), but also revealed an increased dependency on pump activity to maintain excitability (and therefore, presumably, $V_{rest}$) for R669H$^{m/m}$ fibers in normal $K^+$. Consistent with this observation, pump stimulation with salbutamol or with calcitonin

gene–related peptide has previously been shown to increase muscle contractility in $Ba^{2+}$-poisoned muscle (27), which shares many features of HypoPP through blockade of the inward rectifier $K^+$ conductance (16). Conversely, the benefit of the hyperpolarizing effect of the electrogenic pump may be offset by a further reduction of extracellular $K^+$. For example, intra-arterial infusion of epinephrine provoked attacks of weakness in a HypoPP patient (28), whereas in vitro studies of human $Ca_V1.1$ HypoPP fibers for which bulk external $K^+$ was clamped showed enhanced contractility when 1 μM epinephrine was added to fibers bathed in 4.5 mM $K^+$, but triggered weakness in a 1 mM $K^+$ solution (19). These complexities illustrate the need to further dissect the effects of $Na^+/K^+$-ATPase stimulation, $K^+$ homeostasis, and other downstream events of adrenergic signaling, such as $Ca^{2+}$-activated $K^+$ channel activation (29), with regard to regulation of excitability in HypoPP muscle. Our mouse model provides the opportunity to systematically explore these phenomena and identify potential therapeutic strategies.

*Pathogenesis of acute paralytic attacks*. Transient attacks of weakness in HypoPP are known to be the result of an ictal depolarized shift of $V_{rest}$, which inactivates $Na^+$ channels and renders the fiber inexcitable (4). The challenge has been to understand the cause of this depolarization, to link this event mechanistically to hypokalemia, and to understand the role of mutant $Na_V1.4$ and $Ca_V1.1$ channels in this process. A major advance was made with the discovery that missense mutations at arginine residues in the S4 voltage sensors of domain II (including R669H) or domain III create an anomalous pathway for ion conduction (14, 15, 30, 31). This pathway is separate from the central $Na^+$-selective pore and has been called the gating pore, to denote that this is the region through which the voltage sensors translocate in the process of voltage-dependent gating of the channel. All 8 known HypoPP mutations in $Na_V1.4$ are located at arginine residues in S4 voltage-sensor domains (Figure 1A), and gating pore currents have been detected for all 6 mutant channels tested to date (R669H, R672H, R672G, R672C, R672S, and R1132Q). In all cases, the HypoPP gating pore is open at hyperpolarized potentials (less than –40 mV), for which the S4 sensor is biased toward the inward position. The gating pore currents for R/H substitutions are carried by protons (15), whereas the other missense mutations create a cation-nonselective pore (30). Expression studies in oocytes suggest that gating pore currents are small, with amplitudes about 1%–0.1% that of the $Na^+$ current through the conventional pore (14, 15). To our knowledge, the present voltage-clamp studies provide the first measurement for the gating pore current density in a $Na_V1.4$ HypoPP channel expressed in mammalian muscle. The slope conductance of 7 nS/nF (equivalent to 7 $\mu S/cm^2$) was consistent with our estimate of 4 $\mu S/cm^2$ based on heterologous expression in oocytes. In the heterozygous state, as occurs in patients with HypoPP, the gating pore conductance would be about 1% of the total resting membrane conductance. This small inward current was active at $V_{rest}$ and opposed the hyperpolarizing effect of $K^+$ currents (primarily the inward rectifier). The combination of a nonlinear inward rectifier $K^+$ current ($I_{KIR}$) and the inward currents through the leakage conductance in resting muscle creates the possibility of 2 stable $V_{rest}$s (32): one at the familiar hyperpolarized value of –90 mV, and a second depolarized one near –50 mV. Reduction of external $K^+$ diminishes $I_{KIR}$ and thereby favors the depolarized state for $V_{rest}$, which in normal muscle occurs only with severe hypokalemia (i.e., <2 mM). The addition of the gating pore current, conducted by $Na_V1.4$ HypoPP mutant channels, further opposes the outward $I_{KIR}$ current and causes the transition to the depolarized state of $V_{rest}$ to occur at a higher $K^+$, about 2.5–3.0 mM (16–18).

This scenario implicates the gating pore as the source of the depolarizing current and accounts for the low-$K^+$ dependence of the anomalous depolarization with attendant loss of excitability and weakness in HypoPP. A critical question is whether HypoPP mutant $Ca_V1.1$ channels also conduct gating pore currents. The high degree of homology between the voltage sensor domains of $Na_V1.4$ and $Ca_V1.1$, plus the fact that S4 R/X mutations in $K_V$ channels produce gating pore currents (33), imply that HypoPP mutants in $Ca_V1.1$ will also likely support gating pore currents. If HypoPP mutant channels for $Na_V1.4$ and $Ca_V1.1$ both conduct gating pore currents, then this convergence would provide a unifying explanation for why mutations in 2 different voltage-gated cation channels that serve very different functions in skeletal muscle can produce a common clinical phenotype.

Measurements to characterize excitability of $R669H^{+/m}$ fibers revealed additional defects in $Na_V1.4$ function, beyond those attributable to gating pore conductance. Compared with WT soleus, the current clamp responses in $R669H^{+/m}$ muscle showed reduced action potential amplitude, decreased maximal rate of rise, and prolonged duration (Figure 5). Similar changes have been reported for action potentials elicited from biopsied fibers in patients with $Na_V1.4$ HypoPP (13). All of these changes are consistent with a reduction in $Na_V1.4$ channel availability. The difference cannot be attributed to a variation in $V_{rest}$, since a holding current was used to set this value to –85 mV in all fibers. The maximum *dV/dt* during the action potential upstroke was proportional to $Na^+$ current density, and was reduced by 45% for $R669H^{+/m}$ muscle. The enhancement of fast and slow inactivation we previously reported for human R669H expressed in HEK cells (12) would only account for a 19% reduction of availability for the mutant allele at –85 mV. Voltage-clamp studies of $Na^+$ currents in $R669H^{m/m}$ fibers confirmed the same enhancement of slow inactivation, plus enhancement of fast inactivation with –10 mV shift (data not shown). Moreover, at the mRNA level, expression of the WT allele and R669H allele were each 0.7 of the total for WT muscle (Figure 1E). Combining these factors yields a predicted total $Na^+$ current density from the 2 alleles of $(0.7 \times 1) + (0.7 \times 0.81)$, or 1.3× WT control. Even discounting the elevated mRNA levels of each allele to 70% of control in $R669H^{+/m}$ muscle, the predicted $Na^+$ current density would be $(0.5 \times 1) + (0.5 \times 0.81)$, or 0.91× control. Therefore, other factors must be responsible for the low $Na^+$ current density in $R669H^{+/m}$ muscle, such as reduced channel density at the surface membrane or a lower peak open probability for R669H channels. This loss-of-function change for the $Na^+$ current conducted by R669H channels would be compounded by the gating pore defect, which, in the setting of low $K^+$, will depolarize $V_{rest}$ and further reduce $Na^+$ channel availability by inactivation.

*Comparison with the M1592V mouse model of HyperPP*. The specificity of the paralysis phenotype produced by different missense mutations of $Na_V1.4$ is illustrated by comparing the present work with our previously published mouse model of HyperPP with a targeted missense mutation at M1592V (22). Both lines of mice had episodic attacks of weakness, but these were triggered by high $K^+$ (8–10 mM) for M1592V and low $K^+$ (≤ 2 mM) for R669H. Spontaneous recovery of force occurred with the in vitro contraction test for both models, even when the $K^+$ challenge was sustained. However, only the R669H mice had spontaneous, large-amplitude, slow oscillations in

force over minutes. Both mouse models had increased sensitivity to $Na^+/K^+$-ATPase inhibitors, with weakness provoked by 0.5–1.0 μM ouabain even in normal $K^+$. Recovery from an attack was also ouabain sensitive in R669H mice. Prominent electrographic myotonia was recorded from M1592V mice, but was not observed in R669H animals, nor could it be provoked by long-duration current injection in individual fibers. In both animal models, the disease phenotype was more pronounced in the homozygous mutants; however, viability beyond weaning was markedly reduced in the homozygous M1592V mutants, whereas lifespan and reproductive capacity were normal for $R669H^{m/m}$ mice. Histologically, M1592V muscle had a marked predominance of oxidative fibers compared with the mixed glycolytic and oxidative pattern in WT controls, probably as a result of the myotonia. Increased variation in fiber size and central nuclei were seen in $R669H^{+/m}$ fibers, and $R669H^{m/m}$ muscle from older mice had vacuolar changes. In R669H muscle, there was no shift in fiber type, there were no vacuolar changes (even in $R669H^{m/m}$ mice at 1 year of age), and subsarcolemmal aggregates were visualized on Gomori trichrome–stained sections.

The phenotypes for M1592V and R669H mice could easily be distinguished from one another, and from litter-matched WT controls, even by an investigator blinded to genotype, on the basis of provocative testing. The ability to reliably distinguish mouse models on the basis of phenotype demonstrates the robust genotype-phenotype association, in the setting of an isogenic background (129/Sv for R669H; C56BL/6J for M1592V). These muscle phenotypes arise from distinctly different functional defects in the mutant channel proteins. M1592V produces gain-of-function defects with impaired fast and slow inactivation, plus enhanced activation (34, 35). R669H causes a loss of function for the $Na^+$ current via enhanced inactivation, plus a further reduction in current density, and also creates a gating pore selective for protons that conducts inward current at $V_{rest}$ and thereby promotes depolarization.

Collectively, these studies of muscle function by in vitro contraction, force, and CMAP monitoring during in vivo glucose plus insulin challenge; microelectrode recordings of individual fiber excitability; and muscle histology showed that a targeted mutation of $Na_V1.4$ at R669H was a cause of HypoPP. The significance of these observations extends beyond the validation of an animal model, because it was previously thought that the distinctly separate clinical phenotypes of HypoPP and HyperPP were a consequence of underlying mutations in $Ca_V1.1$ and $Na_V1.4$, respectively (5, 7). We now provide an experimental demonstration in an animal model that a missense mutation in $Na_V1.4$ can produce the cardinal features of HypoPP, while also excluding HyperPP features, as demonstrated by the lack of increased susceptibility to weakness with high-$K^+$ challenge or myotonia.

## Methods

*Generation of $Na_V1.4$-R669H knockin mice*. A *Mus musculus* BAC clone (clone-ID, RP24-378D8; Children's Hospital Oakland Research Institute) containing exons 8–15 of *SCN4A* served as a template for the targeting vector to create a knockin mutation by homologous recombination in ES cells (Figure 1). The ortholog of the human HypoPP mutation R669H was created with a CGT→CAC substitution at mouse codon R663 using the QuikChange Mutagenesis kit (Stratagene). 2 silent polymorphisms were introduced at the wobble bases of codons 661 (GTG→GTA) and 662 (CTC→CTG) to create a new ScaI site and to optimize a mutation-specific primer for subsequent validation of the mutant allele. 2 *loxP* sites were also introduced to flank exon 13, where murine R663H resided. Exon numbering began with a transcript contained entirely in the 5′ untranslated region, designated as exon 1 (transcript ID, ENSMUST00000106818). A PGK-driven neomycin resistance cassette flanked by 2 *FRT* sites (a part of pLNeoNsi plasmid) was inserted in intron 12 of *SCN4A* in the targeting construct to serve as an ES cell positive selection marker. A PGK-driven diphtheria toxin cassette was inserted in intron 15 and used for ES cell negative selection. The complete targeting vector in pBlueScript backbone (~22.4 kb) was linearized with SalI prior to electroporation into ES cells in the transgenic core facility at UT Southwestern Medical Center. Diphtheria toxin–resistant ES cells were screened by PCR, and the positive clones were used for blastocyst injection. Male chimeras were bred with 129/Sv strain WT females, and the resulting $R669H^{+/m}$ F1 males were bred with a female 129svflip1 (provided by M. Tallquist, UT Southwestern Medical Center) constitutively expressing Flp recombinase to excise the neomycin resistance cassette.

All animals used in this study were in 129/Sv background, after a minimum of 4 backcrosses with the 129/Sv strain, and in which the intron 12 neomycin gene was deleted. Mice aged 3–6 months were used for the physiological studies.

*Mouse care, grouping, and monitoring*. See Supplemental Methods.

*Genotyping and RNA expression*. Genotyping was performed on tail snip DNA by PCR amplification with an intron 12 forward primer (GCCCTTCGGTCCCCAAAGCCTCTGCCAGG) and the R669H-dn4 reverse primer (CTTTACAGTTTAGCTTCCAAGGGGCCAAGTGG). PCR products were analyzed on a 1% agarose gel to resolve the 400- and 480-bp amplimers from the WT and mutant alleles, respectively.

Total RNA was isolated from freshly dissected gastrocnemius muscle with TRI Reagent BD (Sigma-Aldrich). The cDNAs were synthesized using SuperScript III first-strand synthesis system (Invitrogen) according to the manufacturer's protocol. PCR amplification for 24 cycles was performed with allele-specific forward primers (R669 forward, GGGCCTATCAGTGC TCCGT; H669 forward, GGGCCTATCAGTACTGCAC) and a common reverse primer (ACGGCGAAGATGAAGACGATGATG) using Choice Taq Mastermix DNA polymerase (Denville Scientific Inc.). A control reaction to normalize for template quality was performed by amplification of β-actin (β-actin forward, AAGCTGTGCTATGTTGCCCT; β-actin reverse, AAGCATTTGCGGTGCACGAT). PCR products were analyzed on a 3% NuSieve GTG agarose gel (Cambrex).

*Histological studies*. Mice were anesthetized with isoflurane inhalation and sacrificed by cervical dislocation. Segments of quadriceps muscles were obtained from WT, $R669H^{+/m}$, and $R669H^{m/m}$ animals. Fresh segments were mounted on gum tragacanth, snap-frozen in 2-methyl butane cooled in liquid nitrogen, and submitted for routine histological and enzyme histochemical staining. Frozen blocks were sectioned at 10-μm thicknesses and stained with H&E and Gomori trichrome, and for nicotinamide adenine dehydrogenase-tetrazolium reductase and myoadenylate deaminase activities using standard published procedures (36). Muscle tissue for ultrastructural evaluation was fixed isometrically in 3% phosphate-buffered glutaraldehyde, dehydrated, and embedded in epon-araldite resin. Semithin sections were cut at 1.5-μm thicknesses and evaluated by light microscopy for proper orientation. Resin blocks were sectioned at 200-nm thickness, mounted on a standard copper grid, stained with uranyl acetate–lead citrate, and evaluated using an H7500 Hitachi transmission electron microscope.

*Sodium polystyrene sulfonate pretreatment and whole-blood chemistries*. To reduce baseline serum $K^+$, mice were fed fudge (37) laced with sodium polystyrene sulfonate (Kayexalate; KVK-TECK Inc.), 22% by weight, for 2–4 days. Whole-blood chemistries were performed on samples collected at the beginning and the end of an experiment by retroorbital sampling in a microvette CB300 tube (Sarstedt). Blood glucose level was measured with the OneTouch Basic Blood Glucose Monitoring system (LifeScan). Serum $K^+$ level was determined by a VITROS 250 Chemistry Analyzer at the UT Southwestern Medical Center mouse metabolic phenotyping core.

*Long-term CMAP and force measurements in anesthetized mice*. Mice were anesthetized by intraperitoneal injection of a 10:1 (v/v) mixture of ketamine (10 mg/ml) and xylazine (1 mg/ml) at a dose of 0.1 ml/10 g. The animal was positioned to deliver a constant metered flow of inhalational anesthesia by a vaporizer (SurgiVet) using 0.5% isoflurane mixed with 100% oxygen at 200–400 ml/min as a starting rate. Animals were kept at 37°C using a heat lamp in conjunction with a thermocouple probe (TCAT-2AC controller; Physitemp Instruments Inc.).

Continuous infusion of a glucose plus insulin mixture was used to provoke sequestration of serum $K^+$ in the myoplasm and induce hypokalemia. The jugular vein was cannulated with a 0.64 mm OD PVC microrenathane catheter (Braintree Scientific Inc.) filled with heparinized saline (50 IU/ml). A sterile solution containing 0.2 U/ml pharmaceutical-grade insulin Humulin R (Eli Lilly) and 0.175 g/ml glucose was infused at a rate of 0.5 ml/h using a BSP-99M multispeed syringe pump (Braintree Scientific Inc.). The sciatic nerve was surgically exposed and stimulated with a bipolar hook electrode (Harvard Apparatus) connected to a stimulus isolator (A285; World Precision Instruments). A 0.1-ms stimulus was used to elicit a synchronous discharge of all excitable muscle fibers. CMAP was recorded from a pair of monopolar electromyography electrodes (The Electrode Store) inserted into the soleus or gastrocnemius muscles and connected to an AC-coupled differential amplifier (model no. P511; Grass Instrument Division). Muscle force was simultaneously measured from a stiff transducer (Kent Scientific Corp.) attached to the Achilles tendon. Stimulation and data acquisition were computer controlled with pCLAMP9 software (Molecular Devices) at a sampling rate of 20 kHz.

*In vitro tetanic force measurement*. Mice were anesthetized with isoflurane inhalation and sacrificed by cervical dislocation. The soleus muscle from each hindlimb was rapidly dissected and mounted vertically in an isometric tissue clamp suspended a 25-ml organ bath (Myobath; WPI Inc.) maintained at 37°C. The bath solution was continuously bubbled with a mixture of 95% $O_2$ and 5% $CO_2$ and contained 118 mM NaCl, 4.75 mM KCl, 1.18 mM $MgSO_4$, 2.54 mM $CaCl_2$, 1.18 mM $NaH_2PO_4$, 10 mM glucose, 24.8 mM $NaHCO_3$, 0.02 U/ml insulin (Eli Lilly), and 0.25 μM D-tubocurarine (Sigma-Aldrich). Contractions were elicited by field stimulation with parallel wire electrodes. The isometric muscle length was adjusted to produce a maximal twitch response. Tetanic isometric contractions were evoked by a train of 40 pulses, 2-ms duration, 80 mA, at 100 Hz (A385 Stimulator; WPI Inc.) delivered every 2–5 minutes for a 30- to 60-minute period to allow for stabilization. Test solutions, prewarmed to 37°C and composed of varying concentrations of KCl (1, 2, 3, 8, and 12 mM) and NaCl (122, 121, 120, 115, and 111 mM) to maintain constant monovalent cation concentration, were applied by rapid perfusion of 8 times the bath volume over 1 minute. After 30 minutes, the bath was returned to the control solution with 4.75 mM $K^+$. Tetanic isometric contractions were measured every 2 minutes, under control of pCLAMP8 (Molecular Devices).

*Muscle fiber excitability*. $V_{rest}$ was measured from individual fibers of a soleus whole-muscle in vitro preparation using a sharp microelectrode filled with 3 M KCl. Fibers were maintained at 37°C in the same bath solution as used for in vitro contraction testing. $V_{rest}$ was measured as the initial membrane potential recorded upon fiber impalement. Mean and variance of the $V_{rest}$ measurements were determined by fitting a Gaussian curve to a histogram generated from pooling all measurements. Action potentials were measured from current clamp recordings made with 2 microelectrodes controlled by an Axopatch 2B amplifier. Dantrolene (3 μg/ml) and the skeletal muscle myosin II inhibitor BTS (20 μM) were added to suppress depolarization-induced contractions. Ionic currents were recorded from dissociated flexor digitorum brevis and lumbricale muscle fibers, using a 2-electrode voltage clamp as previously described, except the fibers were not detubulated with glycerol (38). The bath solution contained 100 mM NaOH, 40 mM TEA-OH, 1.5 mM $Ca(OH)_2$, 2.5 mM $Ba(OH)_2$, 1 mM $Co(OH)_2$, 5 mM 4-aminopyridine, 0.001 mM tetrodotoxin, 0.2 mM anthracene-9-carboxylate, 10 mM HEPES, 10 mM glucose, with pH adjusted to 7.4 with methanesulfonic acid. Control experiments in oocytes expressing $Na_V1.4$-R669H demonstrated the gating pore current was not significantly blocked by any components in this bath solution (data not shown). Dantrolene (3 μg/ml) and BTS (20 μM) were added to suppress contraction, and a solution exchange with bath containing 3.5 mM $La(OH)_3$ was used to isolate the gating pore current.

*Statistics*. Data are presented as mean ± SEM. 1-sided ANOVA at the 0.05 level was used to test for a difference of the means among the 3 genotypes. In cases where a difference in the means was present, the post-hoc Bonferroni correction was used to individually test whether $R669H^{+/m}$ or $R669H^{m/m}$ differed from WT. A $P$ value less than 0.05 was considered significant.

*Study approval*. All procedures were in accordance with animal protocols approved by the UT Southwestern Medical Center Institutional Animal Care and Use Committee.

## Acknowledgments

This work was supported by the Muscular Dystrophy Association (MDA 4324) and by NIH grant AR-42703 from NIAMS.

Received for publication February 2, 2011, and accepted in revised form July 13, 2011.

Address correspondence to: Stephen C. Cannon, Department of Neurology, UT Southwestern Medical Center, 5323 Harry Hines Blvd., Dallas, Texas 75390-8813, USA. Phone: 214.645.6225; Fax: 214.645.6239; E-mail: steve.cannon@utsouthwestern.edu.

1. Lehmann–Horn F, Rüdel R, Jurkat–Rott K. Nondystrophic myotonias and periodic paralyses. In: Engel AG, Franzini-Armstrong C, eds. *Myology*. New York, New York, USA: McGraw Hil; 2004:1257–1300.
2. Cannon SC. Pathomechanisms in channelopathies of skeletal muscle and brain. *Annu Rev Neurosci*. 2006;29:387–415.
3. Venance SL, et al. The primary periodic paralyses: diagnosis, pathogenesis and treatment. *Brain*. 2006;129(pt 1):8–17.
4. Rüdel R, Lehmann-Horn F, Ricker K, Kuther G. Hypokalemic periodic paralysis: in vitro investigation of muscle fiber membrane parameters. *Muscle Nerve*. 1984;7(2):110–120.
5. Elbaz A, et al. Hypokalemic periodic paralysis and the dihydropyridine receptor (CACNL1A3): genotype/phenotype correlations for two predominant mutations and evidence for the absence of a founder effect in 16 caucasian families. *Am J Hum Genet*. 1995;56(2):374–380.
6. Resnick JS, Engle WK, Griggs RC, Stam AC. Acetazolamide prophylaxis in hypokalemic periodic paralysis. *N Engl J Med*. 1968;278(11):582–586.
7. Ptacek LJ, et al. Dihydropyridine receptor mutations cause hypokalemic periodic paralysis. *Cell*. 1994;77(6):863–868.
8. Bulman DE, et al. A novel sodium channel mutation in a family with hypokalemic periodic paralysis. *Neurology*. 1999;53(9):1932–1936.
9. Sternberg D, et al. Hypokalaemic periodic paralysis type 2 caused by mutations at codon 672 in the muscle sodium channel gene SCN4A. *Brain*. 2001;124(pt 6):1091–1099.
10. Matthews E, et al. Voltage sensor charge loss accounts for most cases of hypokalemic periodic paralysis. *Neurology*. 2009;72(18):1544–1547.
11. Morrill JA, Brown RH Jr, Cannon SC. Gating of the L-type Ca channel in human skeletal myotubes: an activation defect caused by the hypokalemic periodic paralysis mutation R528H. *J Neurosci*. 1998;18(24):10320–10334.
12. Struyk AF, Scoggan KA, Bulman DE, Cannon SC. The human skeletal muscle Na channel mutation R669H associated with hypokalemic periodic paralysis enhances slow inactivation. *J Neurosci*. 2000;20(23):8610–8617.
13. Jurkat-Rott K, et al. Voltage-sensor sodium channel mutations cause hypokalemic periodic paralysis type 2 by enhanced inactivation and reduced current. *Proc Natl Acad Sci U S A*. 2000; 97(17):9549–9554.
14. Sokolov S, Scheuer T, Catterall WA. Gating pore current in an inherited ion channelopathy. *Nature*. 2007;446(7131):76–78.
15. Struyk AF, Cannon SC. A $Na^+$ channel mutation linked to hypokalemic periodic paralysis exposes a proton-selective gating pore. *J Gen Physiol*. 2007;130(1):11–20.
16. Struyk AF, Cannon SC. Paradoxical depolarization of $Ba^{2+}$- treated muscle exposed to low

extracellular K+: insights into resting potential abnormalities in hypokalemic paralysis. *Muscle Nerve*. 2008;37(3):326–337.
17. Cannon SC. Voltage-sensor mutations in channelopathies of skeletal muscle. *J Physiol*. 2010; 588(pt 11):1887–1895.
18. Jurkat-Rott K, et al. K+-dependent paradoxical membrane depolarization and Na+ overload, major and reversible contributors to weakness by ion channel leaks. *Proc Natl Acad Sci U S A*. 2009; 106(10):4036–4041.
19. Iaizzo PA, Quasthoff S, Lehmann-Horn F. Differential diagnosis of periodic paralysis aided by in vitro myography. *Neuromuscul Disord*. 1995;5(2):115–124.
20. Tricarico D, Capriulo R, Conte Camerino D. Insulin modulation of ATP-sensitive K+ channel of rat skeletal muscle is impaired in the hypokalaemic state. *Pflugers Arch*. 1999;437(2):235–240.
21. Gallant EM. Barium-treated mammalian skeletal muscle: similarities to hypokalemic periodic paralysis. *J Physiol*. 1983;335:577–590.
22. Hayward LJ, et al. Targeted mutation of mouse skeletal muscle sodium channel produces myotonia and potassium-sensitive weakness. *J Clin Invest*. 2008;118(4):1437–1449.
23. Francis D, Farley K, Hayward LJ, Cannon SC. Acetazolamide protects against K-induced weakness in a mouse model of HyperPP. *Ann Neurol*. 2005;58:S36.
24. Francis DG, Rybalchenko V, Struyk A, Cannon SC. Leaky sodium channels from voltage sensor mutations in periodic paralysis, but not paramyotonia. *Neurology*. 2011;76(19):1635–1641.
25. Engel AG. Evolution and content of vacuoles in primary hypokalemic periodic paralysis. *Mayo Clinic Proceedings*. 1970;45(11):774–814.
26. Arzel-Hezode M, et al. Homozygosity for dominant mutations increases severity of muscle channelopathies. *Muscle Nerve*. 2010;41(4):470–477.
27. Clausen T, Overgaard K. The role of K+ channels in the force recovery elicited by Na+-K+ pump stimulation in Ba2+-paralysed rat skeletal muscle. *J Physiol*. 2000;527 pt 2:325–332.
28. Engel AG, Lambert EH, Rosevear JW, Tauxe WN. Clinical and electromyographic studies in a patient with primary hypokalemic periodic paralysis. *Am J Med*. 1965;38:626–640.
29. Geukes Foppen RJ, Siegenbeek Van Heukelom J. Isoprenaline-stimulated differential adrenergic response of K+ channels in skeletal muscle under hypokalaemic conditions. *Pflugers Arch*. 2003;446(2):239–247.
30. Struyk AF, Markin VS, Francis D, Cannon SC. Gating pore currents in DIIS4 mutations of NaV1.4 associated with periodic paralysis: saturation of ion flux and implications for disease pathogenesis. *J Gen Physiol*. 2008;132(4):447–464.
31. Francis DG, Rybalchenko V, Struyk A, Cannon SC. Leaky sodium channels from voltage sensor mutations in periodic paralysis, but not paramyotonia. *Neurology*. 2011;76(19):1635–1641.
32. Siegenbeek van Heukelom J. Role of the anomalous rectifier in determining membrane potentials of mouse muscle fibres at low extracellular K+. *J Physiol*. 1991;434:549–560.
33. Starace DM, Bezanilla F. Histidine scanning mutagenesis of basic residues of the S4 segment of the shaker k+ channel. *J Gen Physiol*. 2001;117(5):469–490.
34. Cannon SC, Brown RH Jr, Corey DP. A sodium channel defect in hyperkalemic periodic paralysis: potassium-induced failure of inactivation. *Neuron*. 1991;6(4):619–626.
35. Hayward LJ, Brown RH Jr, Cannon SC. Slow inactivation differs among mutant Na channels associated with myotonia and periodic paralysis. *Biophys J*. 1997;72(3):1204–1219.
36. Dubovitz V, Sewry CA. *Muscle Biopsy: A Practical Approach*. Atlanta, Georgia, USA: Saunders Elsevier; 2007.
37. Johnson K, Gardner ME. Kayexalate candy. *Am J Hosp Pharm*. 1978;35(9):1034–1035.
38. Fu Y, Struyk A, Markin V, Cannon S. Gating behaviour of sodium currents in adult mouse muscle recorded with an improved two-electrode voltage clamp. *J Physiol*. 2011;589(pt 3):525–546.